11th World Congress on Computational Mechanics (WCCM XI)
5th European Conference on Computational Mechanics (ECCM V)
6th European Conference on Computational Fluid Dynamics (ECFD VI)
E. Oñate, J. Oliver and A. Huerta (Eds)

STUDY OF NONLINEAR FREE-SURFACE SPIKE INDUCED BY BUBBLE

A-MAN ZHANG[*], LI SHUAI [*] AND XIONG-LIANG YAO[*]

[*] Harbin Engineering University
#515 Chuanhai Building, Nantong Street No.145(Harbin Engineering University), Nangang District, Harbin, Heilongjiang Province, China
email: zhangaman2010@gmail.com

Key Words: *Bubble, Free Surface, Crown Spike, Boundary Element Method.*

Abstract. The strong interaction between bubble and free surface is simulated numerically in this paper. A downward Bjerknes jet would form for the case of weak buoyancy force, while a spike would form on the free surface. When the bubble-free-surface distance varies, different kinds of spikes may be observed after the jet impact, among which a "crown" spike was discovered by Zhang A-man in their experiments [Zhang A M, Wang C, Wang S P, Cheng X D 2012. *Acta Phys. Sin.* **61** 084701]. A boundary element method with some numerical techniques is adopted to study this interesting phenomenon. Due to jet impact and liquid compressibility, about 70% system energy would lose when the bubble reaches a minimum volume[Lee M, Klaseboer E, Khoo B C 2007 *J. Fluid Mech.* **570** 407]. Besides, the toroidal bubble keeps moving away from the free surface, which results in a weaker interaction between them. Therefore, the evolution of the toroidal bubble is simulated till its minimum volume is attained. After that, the calculation of the free-surface motion is continued without regard to the effect of bubble. The validation of our numerical model is confirmed by its good agreement with an experiment conducted. Some calculation results are presented to illustrate the formation mechanism and the influence factors of crown spike.

1 INTRODUCTION

The free surface provides a constant-pressure (1 atm.) boundary to a bubble beneath. For the case of weak buoyancy force, a downward jet and an upward spike would form at the collapse phase of the bubble. This phenomenon was firstly observed experimentally by Gibson [1]. Blake and Gibson [2] studied numerically the interaction between bubble and free surface, and they found the same results. Wang [3] used boundary-integral method to study the dynamic behavior of bubble under different conditions. Wang [4] put a vortex ring in the bubble after the jet threading the other side of the bubble, so the toroidal bubble could be simulated. However, the toroidal bubble would split into several small bubbles, which brings many difficulties in numerical simulation. Robinson [5] studied the interaction of two cavitation bubbles with a free surface, and the information on the pressure field surrounding the bubble was provided numerically. In the previous study, much attention was paid on the motion of the bubble while the dynamic behavior of the spike was less cared, especially the

motion after the jet impact.

Zhang [6] used high-speed photography to study different kind of spike induced by a bubble, and they divided the spike into split, splash, crown, tower and mound. These phenomena are rarely studied numerically. The first reason is these phenomena occur after the bubble jet for long, and the second reason is the distance between the bubble and free surface is too small, which results in split and splash. In numerical study, it is difficult to handle the split, splash and multi-oscillations of a bubble. Li [7] and Han [8] studied the later phenomenon of the free surface without taking the influence of the toroidal bubble into consideration, and they found that a crown spike would form with the relative error within 15%.

This paper comes up with a solution to study the crown spike induced by a bubble. The interaction between a bubble and a free surface is simulated by using boundary element method, and the "vortex ring model" is employed to handle the toroidal bubble. The bubble is removed when the bubble reaches its minimum volume or the toroidal bubble is ready to split. Then the later motion of the free surface is simulated without the bubble. The validation of the model is confirmed by comparison with experimental results, and the effect of the distance parameter γ is discussed.

2 THEORY

The liquid surrounding the bubble is assumed inviscid and incompressible, and the motion irrotational [2-5]. Hence, the velocity field $\boldsymbol{u}$ can also be described using potential theory

$$\boldsymbol{u} = \nabla\Phi \tag{1}$$

The velocity potential Φ satisfies the Laplace equation:

$$\nabla^2\Phi = 0 \tag{2}$$

The dynamic boundary condition on the bubble surface and the free surface can be written as [7]

$$\frac{d\Phi}{dt} = \frac{(\nabla\Phi)^2}{2} + \frac{P_{ref}}{\rho} - \frac{P_{out}}{\rho} - gz \tag{3}$$

$$\frac{d\Phi}{dt} = \frac{(\nabla\Phi)^2}{2} - g(z-h) \tag{4}$$

where ρ is the density, P_{ref} is the ambient pressure of the liquid around the bubble, P_{out} is the pressure on the bubble surface, g is the gravity acceleration, h is the distance between the initial-bubble center and the free surface.

The kinematic boundary condition is [5]

$$\frac{d\boldsymbol{X}_i}{dt} = \boldsymbol{u}_i \tag{5}$$

where $\boldsymbol{u}_i$ is the fluid velocity at the point $\boldsymbol{X}_i$.

The solution of (2) may be written in terms of an integral equation [9]

$$\iint_S \left(\frac{1}{|\mathbf{q}-\mathbf{r}|} \cdot \frac{\partial\Phi(\mathbf{q},t)}{\partial n} - \Phi(\mathbf{q},t)\frac{\partial}{\partial n}\left(\frac{1}{|\mathbf{q}-\mathbf{r}|}\right) \right) dS(\mathbf{q}) = \varepsilon(\boldsymbol{r},t)\cdot\Phi(\boldsymbol{r},t) \tag{6}$$

where $\varepsilon(\boldsymbol{r},t)$ is the solid angle of a fixed point $\boldsymbol{r}$ on flow boundaries with the integration variable $\mathbf{q}$ also situated on boundaries, $\partial/\partial n$ is the normal inward derivative from the boundary S. More details in numerical modeling can be found in Blake [2] and Wang [3-4].

The pressure inside the bubble is assumed to be uniform and consists of a constant vapor pressure and a volume-dependent noncondensable gas pressure [10]. Hence, the bubble pressure as a function of the volume is described as

$$P_g = P_c + P_{ini}(V_{ini}/V)^{\vartheta} \tag{7}$$

where the subscript *ini* denotes initial quantities, ϑ is the ratio of the specific heats for the gas, P_c is the vapor pressure.

Consider the jet impacting on the opposite bubble surface, forming a toroidal bubble. To solve this problem, a vortex ring is introduced inside the toroidal bubble [4]. The strength of the vortex ring is the circulation Γ of the flow along a closed path that threads through the torus, which is equal to the jump of the potential across the contact points at the impact time

$$\Gamma = \int_C \mathbf{u}d\mathbf{l} = \Phi_N - \Phi_1 \tag{8}$$

where Φ_N and Φ_1 are the velocity potential at the impact points. The circulation Γ is equal to the jump in the potential at the impact point.

Then, the velocity potential is decomposed into two parts: the potential Φ_v of the vortex ring of strength Γ, and a single-valued remnant potential Φ_r

$$\Phi = \Phi_v + \Phi_r \tag{9}$$

More details about the calculation of Φ_v and Φ_r can refer to Wang [4].

Simultaneously, the velocity of the toroidal bubble $\mathbf{u}_{\mathbf{totol}}$ is decomposed into two parts: the velocity of a circular vortex ring $\mathbf{u}_{\mathbf{v}}$, and the remnant velocity $\nabla\Phi_r$

$$\mathbf{u}_{\mathbf{totol}} = \mathbf{u}_{\mathbf{v}} + \nabla\Phi_r \tag{10}$$

where the velocity of a circular vortex ring $\mathbf{u}_{\mathbf{v}}$ can be calculated from Bio-Savart law

$$\mathbf{u}_{\mathbf{v}}(r,z) = \frac{\Gamma}{4\pi}\int_C \frac{d\mathbf{l}\times\mathbf{r}}{r^3} \tag{11}$$

The dynamic boundary condition for on the bubble surface can be written as

$$\frac{d\Phi_r}{dt} = -\frac{|\mathbf{u}_{\mathbf{totol}}|^2}{2} + \mathbf{u}_{\mathbf{totol}}\cdot\nabla\Phi_r + \frac{P_{ref} - P_{out}}{\rho} - gz \tag{12}$$

Here we have scaled length with respect to the maximum radius which the largest bubble under consideration might achieve in an infinite body of fluid, R_m; pressure by $\Delta P = P_{ref} - P_c$; time by $R_m\sqrt{\rho/\Delta P}$. Besides, some dimensionless parameters are given to describe a bubble:

Strength parameter: $\varepsilon = P_{ini}/\Delta P$

Distance parameter: $\gamma = h/R_m$

Buoyancy parameter: $\delta = (\rho g R_m/\Delta P)^{0.5}$

3 RESULTS AND DISCUSSION

3.1 Comparison between numerical and experimental results

In order to confirm the validation of our model, an experiment from Li [7] is used to make a comparison with numerical result. The maximum radius of the bubble is 13mm, and the

distance between the bubble and the free surface at beginning is 8.1mm. The initial parameter of the bubble is taken as $\varepsilon = 20, \delta = 0.053, \gamma = 0.623$, and the bubble surface is discretized as 100 elements. Figure1 ($a \sim f$) shows the experimental results, and Figure 2 ($a' \sim f'$) shows the numerical results correspondingly. The free surface is pushed upward during the growth of the bubble, and the bubble is also attracted upward slightly by the free surface. As shown in Figure 2 (b'), when the bubble is collapsing, fluid will be drawn rapidly into the region between the bubble and free surface, which leads to the formation of a stagnation point and a high-pressure region along the z-axis [2-3]. The high-pressure region will redirect the incoming flow from the sides to form the downward bubble jet and upward free surface spike. More importantly, the high-pressure region always exists during the collapse of the bubble, which speed up the jet velocity continuously until the jet thread the opposite side of the bubble. The simple-connected bubble transforms into a double-connected bubble, and a vortex ring is put inside the toroidal bubble in the following calculations.

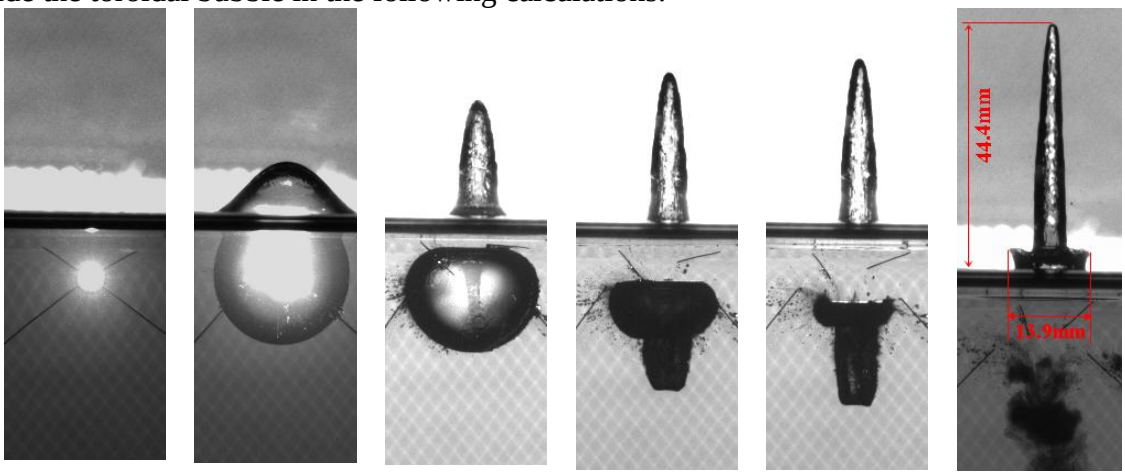

(a) (b) (c) (d) (e) (f)

Figure 1: The interaction between a bubble and free surface (Li 2013) [7]. The nondimensional times are 0, 0.551, 1.241, 1.562, 1.700 and 2.573.

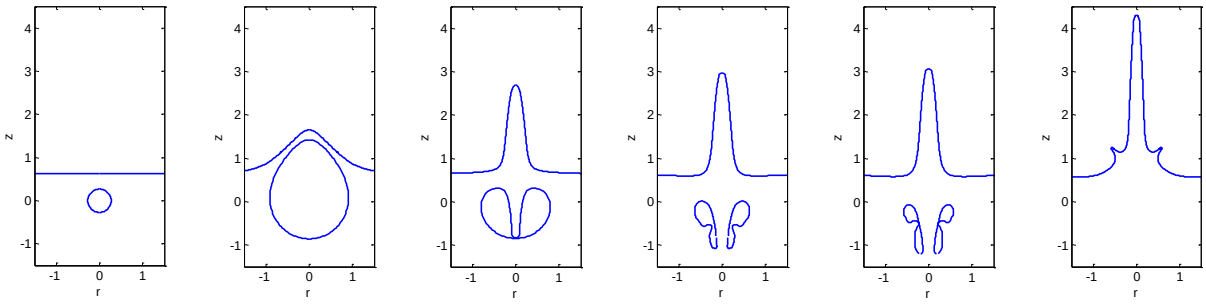

(a') (b') (c') (d') (e') (f')

Figure 2: Evolution of bubble and free surface shapes corresponding to the experiment in Figure 1.Times are the same with Figure 1.

A protrusion appears soon after the jet impact because the velocity of the jet is much greater other part of the bubble surface. In terms of centroid motion, the toroidal bubble moves downward quickly, and a good portion of the bubble is ‘stretched out’ in the vertical

direction. As shown in Figure 1 ($d \sim f$), the bubble moves violently after jet impacting, and the toroidal bubble often breaks into several small bubbles, which can be found in Wang [4], Zhang [6], Li [7], Tong [11] and Pearson [12]. The later motion of the bubble is difficult to model because of the split and splash.

The study of Lee [13] shows that about 70% system energy would lose when the bubble reaches a minimum volume. Tong [11] found shock waves are emitted at a violent splash impact, which will cause much energy loss. Besides, some energy will transform into potential energy during bubble's downward motion. To sum up, the influence of the toroidal bubble on the free surface drops quickly, but the spike will move upward because of inertia. From all discussed above, we come up with a method to handle this problem: the toroidal bubble is removed when it reaches minimum volume or the bubble is ready to split. Although this simple way will bring some errors to our calculation, it is an efficient method to study some characteristic of the crown spike if the error is allowable.

The shape of the spike in calculation (Figure 2 (f')) meets the experimental result (Figure 1 (f)) well. The shape of the spike has changed a lot for it is like an 'imperial crown', so we call it 'crown spike' in this paper. In Figure 1 (f), the height of the spike is 44.4mm; the width of the crown is 13.9mm. In the calculation (Figure 2 (f')), the height of the spike is 47.8mm (relative error: 7.7%); the width of the crown is 15.1mm (relative error: 8.6%). The errors are within 9%, which is mainly caused by the ignorance of the bubble's second period. However, this error is allowable in some cases, so this simple method will be used to study some characteristics of the crown spike in this study.

3.2 Effect of distance parameter γ

It is shown that the distance parameter γ has important effect on bubble motion in the work by Blake [2] and Wang [3]. Experiments conducted by Zhang [6] shows the motion of the free surface has much connection with distance parameter. This section deals with the effect of distance parameter on the characteristics of crown spike. There are five cases will be discussed. The strength parameter and buoyancy parameter are taken as: $\varepsilon = 20, \delta = 0.05$; the distance parameters are taken as: 0.65, 0.75, 0.85 and 0.95, respectively.

Figure 3(a) shows bubble and free surface geometries when the jet impacts on the opposite side of the bubble, the times are 1.297, 1.466, 1.585 and 1.670, respectively. As bubbles are initiated at smaller distances from free surface, the interaction becomes stronger and the time jet impact will decrease. It is obvious that the liquid jet and spike are very narrow for $\gamma = 0.65$. If γ become larger, the liquid jet and spike will increase in width; the spike will decrease in height. The interaction between pre-toroidal bubble and free surface has been numerous studied, so we won't discuss it in detail.

After jet penetration, the toroidal bubble continues to collapse. Figure 3(b) shows toroidal bubble and free surface shapes when bubble reaches minimum volume or begins to split, the times are 1.527, 1.612, 1.675 and 1.715. For $\gamma \le 0.75$, the toroidal bubbles are begin to split; for $\gamma \ge 0.85$, the toroidal bubbles reach their minimum volume. The bubble size then becomes vastly smaller and has little influence on the free surface, so it seems reasonable to remove the bubble from the simulation at this time. Figure 3(c) shows crown spike shapes at t=5. As

bubbles are initiated at smaller distance from the free surface, both the spike and the crown increase in height and decrease in width.

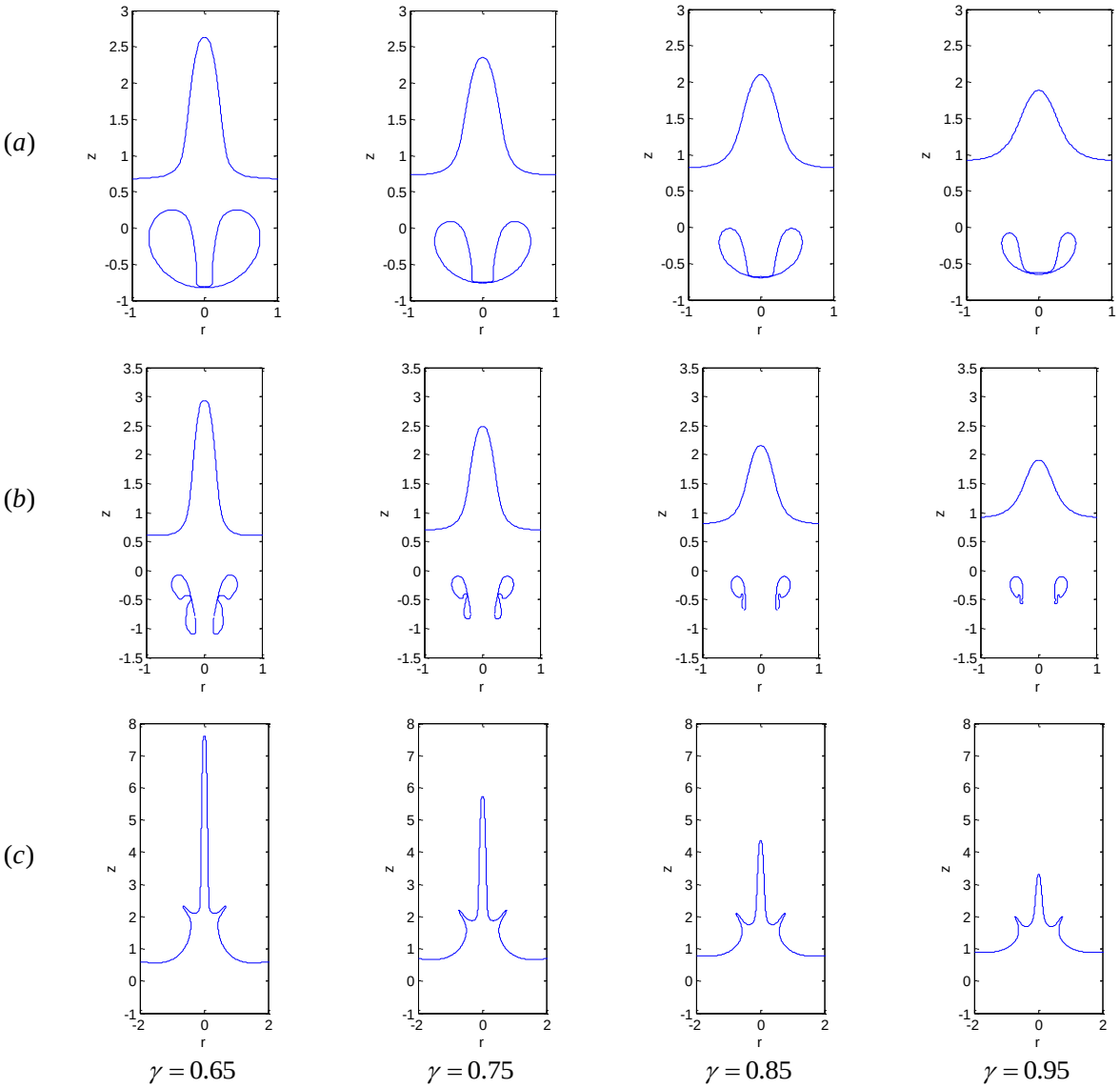

Figure 3: (a) Bubble and free surface shapes when the jet impact on the opposite side of the bubble. Times are 1.297, 1.466, 1.585 and 1.670. (b) Toroidal bubble and free surface shapes when bubble reaches minimum volume or begins to split. Times are 1.527, 1.612, 1.675 and 1.715. (c) Crown spike shapes at t=5.

Figure 4 shows the evolution of the volume of a bubble for a range of distance parameter with the toroidal bubble motion considered. The maximum volume increases as the distance parameter γ is gained, and spends more time. The maximum volume trends to the Reyleigh bubble limit of $4\pi/3$. The evolution of the height of the free surface spike for a range of distance parameter is given in Figure 5. The spikes grow nonlinearly during the early expansion phase of the bubble, and increase almost in a linear mode afterward. Longuet-Higgins [14] noted that a rapid acceleration of the free surface ensues when the angle between the local tangents to the surface falls below the critical angle of 109°, then the spike grows

with constant velocity. This phenomenon was observed in the experiments of Blake and Gibson [15]. From the tendency of the curves in Figure 5, the influence of the removal of toroidal bubble on free surface motion is insignificant.

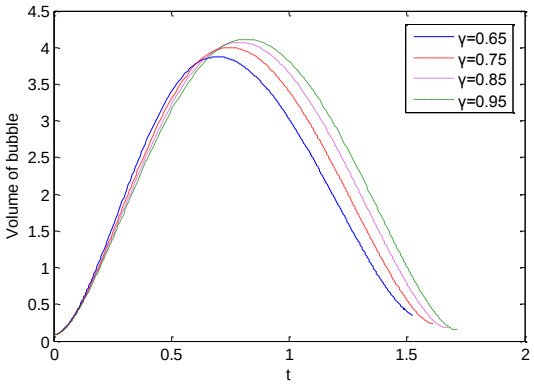

Figure 4: Evolution of the volume of a bubble for a range of distance parameter.

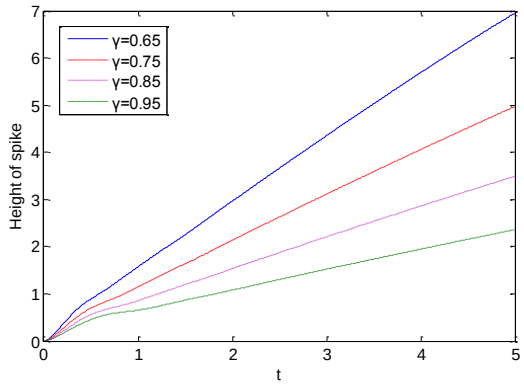

Figure 5: Evolution of the height of the free surface spike for a range of distance parameter.

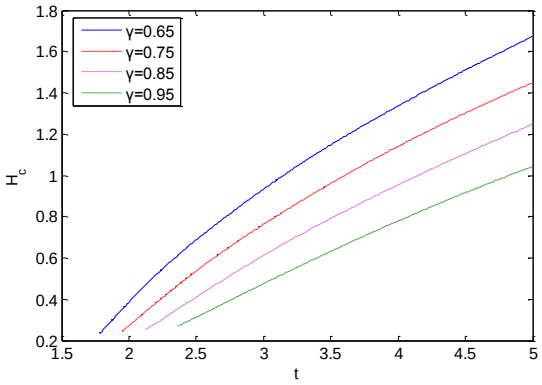

Figure 6: Evolution of the height of the free surface crown for a range of distance parameter.

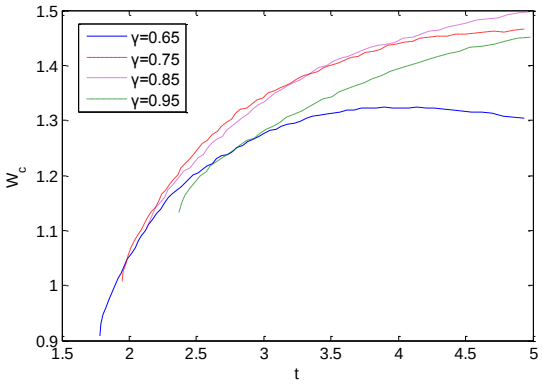

Figure 7: Evolution of the width of the free surface spike for a range of distance parameter.

In Figure 6 we show the evolution of the height of the free surface crown, H_c, for a range of distance parameter γ. Increasing of distance parameter γ will lead to decrease of H_c, but the speed of the crown is not always constant. The emerging time of the crown inceases as the distance parameter is increasing. Figure 7 shows the evolution of the width of the free surface spike, W_c, for a range of distance parameter γ. For $\gamma = 0.65$, the width of the spike increases before $t = 3.9$, and then decreases afterward. Li [7] call this phenomenon "apron-shrink". There is a critical moment, t_c, that divide the motion of the crown into a increase phase and a decrease phase in width. We can note that the critical moment t_c for $\gamma = 0.75$ is larger than $\gamma = 0.65$, and for $\gamma \geq 0.85$, the critical moment is larger than 5.

4 CONCLUSIONS

Based on potential flow theory, boundary element method is employed to study the crown spike induced by weak buoyancy bubble, with the distance parameter $\gamma \in [0.65, 0.95]$. "Vortex ring model" is used to simulate the interaction between toroidal bubbles with free surface. The toroidal bubble is removed when it reaches minimum volume or the bubble is ready to split.

Although this simple way will bring some errors to our calculation, it is an efficient method to study some characteristic of the crown spike, and the error is less than 9%.

1) For distance parameter $\gamma \le 0.75$, toroidal bubble splits before reaching the minimum volume; for distance parameter $\gamma \ge 0.85$, the toroidal bubble reaches its minimum volume before splitting.
2) The spike grows nonlinearly during the early expansion phase of the bubble, and increase almost in a linear mode afterward, and the influence of the removal of toroidal bubble on free surface motion is insignificant.
3) As the distance parameter γ increases, the crown decreases in height, and the emerging time of the crown inceases. There is a critical moment, t_c, that divide the motion of the crown into a increase phase and a decrease phase in width. The critical moment delayed when the bubble initiated further from the free surface.

REFERENCES

[1] Gibson D C 1968 *The Third Australasian Conference on Hydraulic and Fluid Mechanics Sydney*, Australia ,November 25-29,1968 p210
[2] Blake J R, Gibson D C. 1987 *J. Fluid Mech*. **19** 99
[3] Wang Q X, Yeo K S, Khoo B C, Lam K Y 1996 *Theoret. Comput. Fluid Dynamics* **8** 73
[4] Wang Q X, Yeo K S, Khoo B C, Lam K Y 1996 *Computers & Fluids* **25** 607
[5] Robinson P B, Blake J R, Kodama T, et al. 2001 *Journal of Applied Physics.*, **89** 8225
[6] Zhang A M, Wang C, Wang S P, Cheng X D 2012 *Acta Phys. Sin.* **61** 084701
[7] Li S, Zhang A M, Wang S P 2013 *Acta Phys. Sin.* **62** 194703
[8] Han R, Zhang A M, Li S 2014 *Chin. Phys. B* **23** 034703
[9] Newman J N 1977 Marine Hydrodynamics (1st Ed.) (London :MIT Press) p131
[10] Best J P 1993 *J. Fluid Mech.* **251** 79
[11] Tong R P, Schiffers W P, Shaw S J, et al. 1999 *J. Fluid Mech.* **380** 339
[12] Pearson A, Cox E, Blake J R, Otto S R 2004 *Eng. Anal. Bound. Elem.***28** 295
[13] Lee M, Klaseboer E, Khoo B C 2007 *J. Fluid Mech.* **570** 407
[14] Longuet-Higgins M S. 1983 *J. Fluid Mech.* **127** 103
[15] Blake J R, Gibson D C. 1981 *J. Fluid Mech.* **111** 123